



島根大学学術情報リポジトリ  
S W A N  
Shimane University Web Archives of kNowledge

Title

The Binding of A $\beta$ 1–42 to Lipid Rafts of RBC is Enhanced by Dietary Docosahexaenoic Acid in Rats: Implicates to Alzheimer's Disease

Author(s)

Michio Hashimoto, Shahdat Hossain, Masanori Katakura, Abdullah Al Mamun, Osamu Shido

Journal

Biochimica et Biophysica Acta (BBA) - Biomembranes, Volume 1848, Issue 6

Published

30 July 2014

URL

<https://doi.org/10.1016/j.bbamem.2015.03.008>

この論文は出版社版ではありません。  
引用の際には出版社版をご確認のうえご利用ください。

**The Binding of A $\beta$ <sub>1-42</sub> to Lipid Rafts of RBC is Enhanced by Dietary Docosahexaenoic Acid in Rats: Implicates to Alzheimer's Disease**

Michio Hashimoto<sup>1†\*</sup>, Shahdat Hossain<sup>1,2†</sup>, Masanori Katakura<sup>1</sup>, Abdullah Al Mamun<sup>1</sup>, Osamu Shido<sup>1</sup>

<sup>1</sup> Department of Environmental Physiology, Shimane University Faculty of Medicine, Izumo, Shimane 693-8501, Japan

<sup>2</sup> Department of Biochemistry & Molecular Biology, Jahangirnagar University, Savar, Dhaka-1342, Bangladesh

<sup>†</sup>These authors contributed equally to the work

\* Corresponding author at: Michio Hashimoto,

Department of Environmental Physiology, Shimane University Faculty of Medicine, Izumo 693-8501, Japan; e-mail address: michio1@med.shimane-u.ac.jp.

*Abbreviations:*

AD, Alzheimer's disease; A $\beta$ s, Amyloid  $\beta$  peptides; BW, body weight; DHA, docosahexaenoic acid; DRMs, detergent-resistant membranes; D $\tau$ , diffusion time; FCS, fluorescence correlation spectroscopy; FM, fluorescence microscope; Hb, hemoglobin; HFIP, hexafluoroisopropylalcohol; LPO, lipid peroxide; RBCs, red blood cells; ROS, reactive oxygen species; TEM, transmission electron microscope; ThT, thioflavin T

## Abstract

Once amyloid  $\beta$  peptides ( $A\beta$ s) of the Alzheimer's disease (AD) build up in blood circulation, they are capable of binding to red blood cell (RBC) and inducing hemolysis of RBC. The mechanisms of the interactions between RBC and  $A\beta$  are largely unknown; however, it is very important for the therapeutic target of  $A\beta$ -induced hemolysis. In the present study, we investigated whether  $A\beta_{1-42}$  interacts with caveolin-1-containing detergent-resistant membranes (DRMs) of RBC and whether the interaction could be modulated by dietary pre-administration of docosahexaenoic acid (DHA). DHA pre-administration to rats inhibited hemolysis by  $A\beta_{1-42}$ . This activity was accompanied by increased DHA levels and membrane fluidity and decreased cholesterol level, lipid peroxidation, and reactive oxygen species in the RBCs of the DHA-pretreated rats, suggesting that the antioxidative property of DHA may rescue RBCs from oxidative damage by  $A\beta_{1-42}$ . The level of caveolin-1 was augmented in the DRMs of DHA-pretreated rats. Binding between  $A\beta_{1-42}$  and DRMs of RBC significantly increased in DHA-rats. When fluorescently labeled  $A\beta_{1-42}$  (TAMRA- $A\beta_{1-42}$ ) was directly infused into the bloodstream, it again occupied the caveolin-1-containing DRMs of the RBCs from the DHA-rats to a greater extent, indicating that circulating  $A\beta$ s interact with the caveolin-1-rich lipid rafts of DRMs and the interaction is stronger in the DHA-enriched RBCs. The levels of TAMRA- $A\beta_{1-42}$  also increased in liver DRMs, whereas it decreased in plasma of DHA-pretreated rats. DHA might help clearance of circulating  $A\beta$ s by increased lipid raft-dependent degradation pathways and implicate to therapies in Alzheimer's disease.

## Highlights

1.  $A\beta_{1-42}$  interacts with caveolin-1-containing detergent-resistant membranes of RBC.
2. DHA pre-administration to rats inhibited RBC hemolysis by  $A\beta_{1-42}$ .

3. The antioxidative property of DHA may rescue RBCs from oxidative damage by A $\beta$ <sub>1-42</sub>.
4. The interaction of A $\beta$ s with the caveolin-1 is stronger in the DHA-enriched RBCs.
5. DHA might help clearance of A $\beta$ s by increased RBC lipid raft-dependent degradation.

**Key Words:** Alzheimer's disease, docosahexaenoic acid, lipid rafts, caveolin-1

## 1. Introduction

Amyloid beta peptides ( $A\beta$ s) are central to the pathogenesis of Alzheimer's disease (AD). The presence of  $A\beta$ s in the plasma membranes of red blood cells (RBCs) has recently attracted great interest because it may be useful as a potential peripheral biomarker for diagnosis of AD [1]. RBC membranes in AD patients are injured by unavoidable exposure to  $A\beta_{1-42}$ , suggesting an increased potential for breakdown of erythrocytes with liberation of hemoglobin (Hb) in the blood, called hemolysis [2,3]. Degradations or dysfunctions of RBCs reduce the delivery of oxygen to the brain. Kiko et al. [1] reported that human RBC  $A\beta_{1-40}$  and  $A\beta_{1-42}$  levels increased and accumulated phospholipid hydroperoxides with aging and  $A\beta$ s levels and accumulation of phospholipid hydroperoxides were decreased by antioxidant supplementation. However, the mechanism(s) by which  $A\beta$  interacts with RBCs remains largely unexplored.

Mature RBCs are devoid of receptor-mediated endocytosis because they lack endocytic machinery [4]. Thus, it is very likely that the receptor-independent docking of circulating  $A\beta$ s occurs on the RBC membrane, which affects the morphology and functions of RBC, as reported in AD patients [1-3, 5-7]. We hypothesize that  $A\beta$ s affect RBCs via caveolin-1-rich lipid rafts and/or caveolae. These microdomains are implicated in a variety of signaling processes in cells [8-10]. The lipid rafts can be functionally isolated as detergent-resistant membranes (DRMs) [11]. In the present study we investigated whether  $A\beta_{1-42}$  binds with DRMs isolated from RBC ghosts. Considering that lipid raft size is well below the resolution limit of conventional microscopy [12], to characterize the binding property of  $A\beta_{1-42}$  with DRMs we used fluorescence correlation spectroscopy (FCS), a highly sensitive method capable of single-molecule detection. FCS measures diffusion time ( $D\tau$ ) of fluorescent probes in the confocal volume. Because higher molecular weight increases the  $D\tau$  across the confocal volume, the observed  $D\tau$  of free probe is much faster than that of probe bound to

lipid rafts [13-15]. In this study, 5-carboxytetramethylrhodamine-labeled  $A\beta_{1-42}$  (TAMRA- $A\beta_{1-42}$ ) was used as a fluorescent probe and mixed with DRMs to monitor  $D\tau$ . In addition, TAMRA- $A\beta_{1-42}$  was infused directly into rat blood to determine whether TAMRA- $A\beta_{1-42}$  localizes in DRMs of RBCs, with concurrent determination of the levels of TAMRA- $A\beta_{1-42}$  in the blood and liver.

Docosahexaenoic acid (DHA, C22:6 n-3) levels are remarkably reduced in RBC membranes of AD patients [16]. DHA supplementation ameliorates cognitive deficits and the brain amyloid burden of  $A\beta$ -infused AD rat models [17-19]. DHA decreases membrane cholesterol levels, affects fatty acid composition, and enhances antioxidative capability. These reports indicate that DHA changes membrane properties. In this study, to examine whether the binding between  $A\beta_{1-42}$  and DRMs could be affected by oral administration of DHA to rats, RBCs from DHA pre-administered rats were incubated with  $A\beta_{1-42}$ , followed by hemolysis monitoring, fatty acid composition analysis, and oxidative state analysis. DRMs from RBC ghosts were used to perform assays of binding of  $A\beta$ s by FCS and determine levels of caveolin-1.

## 2. Materials and Methods

### 2.1. Animals

Wistar rats (generation 0, G0) (Jcl: Wistar; Clea Japan) were housed, bred, and maintained on a fish oil-deficient diet (F-1<sup>®</sup>; Funabashi Farm) and water ad libitum. Inbred 2<sup>nd</sup>-generation male rats (25 weeks old, 300–400 g body weight, [BW]) fed the same F-1 diet, were randomly divided into two groups: the DHA group (n = 10) and the F1 control group (n = 10). The DHA group was orally administered ethyl-ester 4,7,10,13,16,19-docosahexaenoate (Harima Foods, Inc., Osaka, Japan) emulsified in 5% gum Arabic solution at 300 mg/kg BW/day, and the control group was orally administered the same volume of 5% gum Arabic

solution alone. Oral administration of DHA emulsion and/or gum Arabic solution was continued for 12 weeks.

All experiments were carried out in accordance with the Guiding Principles for the Care and Use of Animals in the Field of Physiological Science of the Physiological Society of Japan and approved by the institutional the Animal Care and Use Committee at Shimane University.

## 2.2. RBC preparation

After deep anesthesia with pentobarbital (50 mg/kg BW), whole blood from individual rats was collected from the inferior vena cava with a heparinized syringe. Half of the blood was used for preparation of plasma and the other half was mixed with Locke's solution (154 mM NaCl, 5.6 mM KCl, 2.3 mM CaCl<sub>2</sub>, 1 mM MgCl<sub>2</sub>, 3.6 mM NaHCO<sub>3</sub>, 5 mM glucose, and 5 mM HEPES; pH 7.2) and pelleted at 300 g for 10 min in plastic tubes. The supernatant was discarded and the RBCs were washed three times with the same solution. The buffy coat and a portion of the upper layer of the RBCs were removed in each wash. The remaining RBCs were immediately subjected to hemolysis assay or used for preparation of DRMs from ghost membranes.

## 2.3. Preparation of A $\beta$ <sub>1-42</sub> peptides and hemolysis assay

Because the A $\beta$ <sub>1-42</sub> displays an extraordinary aggregation propensity in aqueous buffer, both unlabeled A $\beta$ <sub>1-42</sub> and TAMRA-A $\beta$ <sub>1-42</sub> were reconstituted initially to a concentration of 0.5 mM in hexafluoroisopropylalcohol (HFIP) to retain their monomeric state, and then stored at -80°C. Before use, HFIP was removed from the aliquots by blowing with N<sub>2</sub> gas, and the A $\beta$ <sub>1-42</sub> was then mixed immediately with Locke's buffer. Then, RBCs (10<sup>7</sup> cells) suspended in 100  $\mu$ l Locke's buffer were mixed with the amyloid solution to a final

concentration of 20  $\mu\text{M}$   $\text{A}\beta_{1-42}$  or TAMRA- $\text{A}\beta_{1-42}$  as desired. RBC hemolysis was quantified by pelleting RBCs at 300  $g$  for 10 min and determining the amounts of Hb released into the supernatant by quantifying absorbance of Hb at 405 nm;  $\alpha$ -tocopherol was used as antioxidant during  $\text{A}\beta$ -induced RBC hemolysis. Aliquots of 5  $\mu\text{L}$  of the  $\text{A}\beta_{1-42}$ -induced hemolysis samples were subjected to confocal laser microscopy to visualize the RBC morphology and the localization of the TAMRA- $\text{A}\beta_{1-42}$ .

#### 2.4. $\text{A}\beta_{1-42}$ fibrillation

$\text{A}\beta_{1-42}$  fibrillation was assayed by thioflavin T (ThT) fluorescence spectroscopy as described [19, 20] previously (see Supplementary file 1).

#### 2.5. Preparation of RBC ghost and DRMs

Washed RBCs were suspended in 40 volumes of ice-cold 5 mM Tris-HCl buffer (pH 7.0), containing 1 mM EDTA and centrifuged (18,000  $g$  at 4°C for 90 min). The supernatant was discarded and centrifugation at 30,000  $g$  and 4°C and washing were repeated until the ghost membranes became whitish. Ghost membranes were stored at -80°C and/or extracted for DRMs. The detergent extraction of RBC ghosts was performed as described previously [21-23] (see Supplementary file 2).

#### 2.6. Binding assay

The purpose of the TAMRA- $\text{A}\beta_{1-42}$  binding assay is to demonstrate that  $\text{A}\beta$ -receptors/target sites are present in reasonable numbers in the DRMs isolated from RBC ghosts and are functioning with appropriate affinity for the TAMRA- $\text{A}\beta_{1-42}$ . The competitive binding experiment measured the ability of increasing concentrations of unlabeled  $\text{A}\beta_{1-42}$  to displace a single concentration of TAMRA- $\text{A}\beta_{1-42}$  from the  $\text{A}\beta$ -receptor/target sites. In brief,

the 10  $\mu\text{g}$  protein of DRMs in 100  $\mu\text{L}$  mixed with 5 nM (100  $\mu\text{L}$ ) of TAMRA- $\text{A}\beta_{1-42}$  were combined with increasing concentrations of unlabeled  $\text{A}\beta_{1-42}$  (0–10  $\mu\text{M}$ ). After a brief flush of  $\text{N}_2$ -gas, the mixture was incubated at 37°C for 12 h to allow receptor/target site binding of the  $\text{A}\beta$ s to reach equilibrium. The assay tubes then were centrifuged to pellet the DRMs.  $\text{A}\beta$  bound to the receptor/target site will be retained in the DRM pellet, whereas unbound  $\text{A}\beta$  will remain in the supernatant. One portion of the pelleted DRMs was used for TAMRA- $\text{A}\beta_{1-42}$  assay using a spectrofluorometer and the other portion was used for the determination of unlabeled  $\text{A}\beta_{1-42}$  by ELISA (see Supplementary file 3).

### 2.7. Immunofluorescence and transmission electron microscopy

TAMRA- $\text{A}\beta_{1-42}$  saturated binding DRMs samples were subjected to fluorescence laser microscopy to determine whether the TAMRA- $\text{A}\beta_{1-42}$  is bound to the surface and/or trapped inside the DRMs. Competitive binding assay samples of DRMs (5  $\mu\text{L}$ ) were placed on a copper grid and stained with 1% uranyl acetate, washed with distilled water, air dried, and examined under a Hitachi H-7000 transmission electron microscope (TEM) with an operating voltage of 75 kV.

### 2.8. ELISA

The amount of unlabeled  $\text{A}\beta_{1-42}$  bound with the DRMs was measured as previously described [20,24]. The levels of caveolin-1 in the DRMs and cathepsin D in RBC ghosts also were measured by ELISA (see Supplementary file 3). The levels of  $\text{A}\beta_{1-42}$  were calibrated using standard  $\text{A}\beta_{1-42}$  solutions. The standard curve was linear in the range of 0–400 pmol/100  $\mu\text{l}$ /well. The absorbance of the control samples was 4–5-fold higher than that of the background (blank) during the ELISAs for caveolin 1 and cathepsin D; therefore, the results were reliable.

### 2.9. Fluorescence Correlation Spectroscopy (FCS)

FCS was performed with a confocal volume element of 1 fL using a Fluoro Point Light apparatus (Olympus, Tokyo, Japan). TAMRA and TAMRA-A $\beta$ <sub>1-42</sub> were used as reference dyes. Each sample (10  $\mu$ g of DRM protein in 50  $\mu$ L of 5 nM TAMRA-A $\beta$ <sub>1-42</sub>) was monitored at room temperature. When the volume element is projected onto the DRMs surface, not only the bound TAMRA-A $\beta$ <sub>1-42</sub> diffusing at the DRM surface but also the unbound TAMRA-A $\beta$ <sub>1-42</sub> will be illuminated; thus, permitting the detection of both slowly and rapidly moving amyloid species. The sample solution initially contained A $\beta$  monomer, which diffused rapidly and freely.

The sample solution after incubation contained A $\beta$  bound to target sites of DRMs, and the A $\beta$  polymerized and formed larger masses that diffused slowly. The diffusion times of these types of A $\beta$  can be readily distinguished with reference dyes; therefore, without any prior assumption regarding the assembly types present in solution, the relative abundance and diffusion time of assembled species can be inferred. Differences in the diffusion times of A $\beta$  in DRMs of RBCs isolated from control and DHA rats were attributable to alterations in the masses of the A $\beta$  species, which could not have been formed without an increased abundance in DRMs of RBCs. The details of principles of FCS data evaluation are described in the Supplementary file 4.

### 2.10. Other *in vitro* methods

Membrane fluidity of DRMs, fatty acid compositions and cholesterol levels in RBC ghosts and DRMs, lipid peroxide (LPO) of DRMs, reactive oxygen species (ROS) of RBC ghosts, and reduced glutathione (GSH) of whole RBCs were determined as previously described [25-27], and are briefly described in the in the Supplementary file 5.

### 2.11. *In vivo* infusion of TAMRA-A $\beta_{1-42}$

TAMRA-A $\beta_{1-42}$  was infused into blood to determine whether TAMRA-A $\beta_{1-42}$  is localized in the DRMs of RBCs and/or TAMRA-A $\beta_{1-42}$  occupancies of DRMs are modulated by the pre-administration of DHA. After pentobarbital anesthesia, 2.0 mL of blood was initially drawn from veins prior to infusion. Immediately after removing HFIP from the TAMRA-A $\beta_{1-42}$  aliquots using N<sub>2</sub> gas, sterile buffer was added, the samples were sonicated briefly (approximately 2 s), and then infused into the blood immediately. TAMRA-A $\beta_{1-42}$  (100 pmol) was infused through the left carotid veins and the incision was closed. After 1 h the rats were sacrificed by bleeding, and levels of TAMRA-A $\beta_{1-42}$  in plasma, DRMs of RBC ghosts, and liver were determined. Protein concentrations were determined with a bicinchoninic acid protein assay kit (Pierce Biotechnology, Rockford, IL).

### 2.12. *Statistical analysis*

Data are presented as mean  $\pm$  standard error of the mean (SEM) from at least three independent experiments. When necessary, one-way ANOVA followed by Bonferroni's post hoc tests was used. Values different at  $P < 0.05$  were considered significantly different.

## 3. Results

### 3.1. *Fibrillation of A $\beta_{1-42}$ in the Locke's solution used for hemolysis*

The formation of amyloid fibrils frequently relies upon the characteristics of the buffers used for the fibrillation process. We accordingly investigated whether A $\beta_{1-42}$  underwent fibrillation processes in Locke's solution (see Supplementary file 1), A $\beta_{1-42}$  fibers were clearly generated in the solution, suggesting that fibrillogenesis definitely ensued in the Locke's hemolysis solution. In the preliminary hemolysis experiments, RBCs were incubated with (procedure i) pre-formed A $\beta_{1-42}$  oligomers, (procedure ii) pre-formed mature A $\beta_{1-42}$

fibers, and (procedure iii) A $\beta_{1-42}$  monomers (immediately after HFIP was removed from the aliquots). The pre-formed oligomers induced hemolysis, whereas the fibers did not (data not shown). In addition, procedure iii helped induced significant hemolysis, suggesting that the “on-pathway” intermediate oligomeric species that emerged during the fibrillation of monomers to fibers in the hemolysis buffer were toxic and exerted hemolytic effects on RBCs (20). Procedure iii helped maintain the oligomeric species in a more functionally, physically, and conformationally uninterrupted and naïve state, as well as avoid the time-consuming and sensitive preparation of oligomers while affording reproducible results.

### *3.2. Effects of pre-administered DHA on A $\beta$ -induced hemolysis of RBC*

A $\beta_{1-42}$  induced hemolysis, and this induction was significantly reduced in the presence of  $\alpha$ -tocopherol (see Supplementary file 6, Fig S2E). The hemolysis induced by A $\beta_{1-42}$  was significantly lower in the RBCs from the DHA-pretreated rats than that in the control rats. The alleviation of hemolysis was accompanied by increased levels of GSH in intact RBCs and decreased ROS in the RBC ghosts, and decreased levels of LPO in the DRMs of DHA-pretreated rats. The levels of cathepsin D were also significantly higher in the ghost membranes of the DHA-pretreated rats (Supplementary file 6).

### *3.3. Effects of pre-administered DHA on RBC ghosts and DRM lipid profiles*

Lipid rafts are defined as cholesterol- and sphingolipid-rich domains, and manipulations of the levels of these lipids can be used to ascertain raft function. The oral administration of DHA for 12 weeks significantly increased the levels of DHA and decreased the levels of cholesterol in whole ghosts and DRMs (Table 1). The levels of plasma DHA were also significantly increased, as expected.



### 3.4. Effect of $A\beta$ on RBC morphology

After it was confirmed that the process of fibrillation of  $A\beta_{1-42}$  occurred in the hemolysis buffer, RBC suspensions were co-incubated with or without freshly prepared monomeric  $A\beta_{1-42}$  to investigate the interactions between  $A\beta$  and intact RBCs on the morphological level. Microscopy revealed numerous blobs, bulges, and diffused membranes with multiple leaks in the  $A\beta_{1-42}$ -treated RBCs (Figure 1, panel1, B, inset B1). In contrast,  $A\beta_{1-42}$ -untreated RBCs exhibited clear demarcations of their membranes (Figure 1, panel1, A, inset A1). The results were consistent with increased hemolysis by  $A\beta_{1-42}$  (see Supplementary file 6). When RBCs were incubated with fluorescently labeled TAMRA- $A\beta_{1-42}$ , they also underwent hemolysis similar to those with unlabeled  $A\beta_{1-42}$ . TAMRA- $A\beta_{1-42}$  was found in the vicinity and/or on the surface of plasma membranes of the RBCs (Figure 1, panel1, C, D, and E). The preadministration of DHA resisted the  $A\beta_{1-42}$ -induced hemolysis of RBCs (Figure 1, panel1, F).

### 3.5. Morphology and interactions of DRMs with TAMRA- $A\beta_{1-42}$

Differential interference contrast microscopy revealed that the milky white RBC ghost suspension consisted of empty sacs, which resembled swollen red cells in form and size (see Supplementary file 7, Fig S3A and its inset). In addition, DRMs spontaneously formed resealed empty membranous sacs and appeared as swollen red cells in differential interference contrast microscopic field (see Supplementary file 7, S3B and its inset). TEM also showed that the DRMs were vesicle-like structures with clear cut membrane bilayer architectures (see Supplementary file 7, S3C).

The DRMs sacs remained intact in the solution and were used for the binding assay of TAMRA- $A\beta_{1-42}$ /unlabeled  $A\beta_{1-42}$ , FCS assay and caveolin-1 measurement. Fluorescence observation demonstrated that TAMRA- $A\beta_{1-42}$  was discernible at the surface and/or inside

the DRM structures (Figure 1, panel2). These results were, at least partially, qualitatively consistent with TEM, where some twisting and ribbon-like  $A\beta_{1-42}$  fibers were evident at the surface and/or inside the DRM sacs (Figure 1, panel3). The possibility that DHA affects the binding of TAMRA- $A\beta_{1-42}$  was tested by measuring the amounts of TAMRA- $A\beta_{1-42}$  that were bound to DRMs of both the F1 control and DHA RBCs.

The effects of DHA on the binding of  $A\beta_{1-42}$  to DRMs of RBCs are shown in Fig. 2, panel 1. The saturation of the binding of TAMRA- $A\beta_{1-42}$  to DRMs reached a concentration of 5–10 nM (Fig. 2A, panel 1). A 5 nM TAMRA- $A\beta_{1-42}$  was used, and then the effect of DHA on the occupancy of TAMRA- $A\beta_{1-42}$  on DRMs was evaluated. DRMs on the RBCs of DHA rats had a significantly increased occupancy of TAMRA- $A\beta_{1-42}$  as compared with those from control rats (Fig. 2B, panel 1). To examine whether the binding to DRMs was specific to  $A\beta$ , the competitive binding of TAMRA- $A\beta_{1-42}$  (5 nM) to DRMs vesicles in the presence of increasing concentrations (0–10  $\mu$ M) of unlabeled  $A\beta_{1-42}$  was examined.

Competition studies revealed that the amount of bound labeled TAMRA- $A\beta_{1-42}$  was reduced significantly by the addition of unlabeled  $A\beta_{1-42}$  (0–10  $\mu$ M). With increasing concentrations of unlabeled  $A\beta_{1-42}$ , the amount of unlabeled  $A\beta_{1-42}$  measured by ELISA also increased, suggesting that the binding of  $A\beta_{1-42}$  to the DRMs was specific. Therefore, TAMRA  $A\beta_{1-42}$  was displaced from the binding/target sites on DRMs by unlabeled  $A\beta_{1-42}$ . Statistically significant increases were found with 3 and 10  $\mu$ M  $A\beta_{1-42}$  (Fig. 2C, panel 1). The DHA-enriched DRMs bound more unlabeled  $A\beta_{1-42}$ , as measured by ELISA. The affinity of the  $A\beta$  for DRMs was also calculated by fitting the data to a one-site-competition equation analysis, which revealed  $EC_{50}$  values of 9.55 and 6.78 nM, respectively, in the DRMs of F1 control and DHA rats. Competition studies showed that the amounts of labeled  $A\beta_{1-42}$  (TAMRA- $A\beta_{1-42}$ ) were significantly reduced by the addition of unlabeled  $A\beta_{1-42}$  (0–10  $\mu$ M). Accordingly, the amount of unlabeled  $A\beta_{1-42}$  measured by ELISA was increased significantly

with the addition of fixed amount of labeled  $A\beta_{1-42}$ , suggesting that the binding of  $A\beta_{1-42}$  to the DRMs was specific. (Fig 2C, panel 1).

The DHA-enriched DRMs had more (displaced) unlabeled  $A\beta_{1-42}$ , as measured by ELISA. The affinity of the Abetas for DRMs was also calculated by fitting the data to a one-site-competition equation [ $Y = \text{Bottom} + (\text{Top} - \text{Bottom}/(1+10^{(X-\text{LogEC}_{50})})$ ], where  $X = \log$  (concentration) and  $Y = \text{bound/unbound}$ . The analysis revealed  $EC_{50}$  values of 9.55 and 6.78 nM, respectively, in the DRMs of F1 control and DHA rats (Fig 2D, panel1).

### 3.6. FCS

Free TAMRA- $A\beta_{1-42}$  in solution and TAMRA- $A\beta_{1-42}$  bound to DRMs were observed by FCS. TAMRA diffused at approximately 100  $\mu\text{s}$  (Fig 1, panel2 A), whereas TAMRA- $A\beta_{1-42}$  alone (in the free form in solution) diffused at approximately 260  $\mu\text{s}$ . However, when the TAMRA- $A\beta_{1-42}$  was added to the DRMs, it exhibited two distinct, fast ( $\tau_1$ ) and slow ( $\tau_2$ ), diffusion times.  $\tau_1$  reflects the diffusion of the free form in solution from DRMs ( $\tau_1$  was considered at approximately 260  $\mu\text{s}$ ) and  $\tau_2$  reflects diffusion of TAMRA- $A\beta_{1-42}$  bound to DRMs. Based on fluorescence intensity fluctuations, the calculated  $\tau_2$  values were  $3228 \pm 300$  and  $3485 \pm 285$   $\mu\text{s}$  in the DRMs of control and DHA-pretreated rats, respectively. The values in the DHA group ( $3485 \pm 285$   $\mu\text{s}$ ) tended to be significantly ( $P = 0.07$ ) higher than those in the F1 control group. This reflects an increased  $A\beta$  aggregation mass and/or increased accumulation of TAMRA- $A\beta_{1-42}$  with a resulting increased time for crossing the volume element projected in the lipid rafts of DHA RBCs. (Fig 2, panel2, B).

### 3.7. Effect of DHA pre-administration on the caveolin-1 levels in the DRMs

As shown in Figure 3A, in DRM fractions the levels of caveolin-1 were also higher in the DRMs of DHA-pretreated rats. The highest increases were found in fraction 3; that is, in the

interface of a 35-40% sucrose solution, indicating the asymmetric distribution of caveolin-1 in DRMs (Figure 3B).

### *3.8. Effect of DHA pre-administration on plasma, RBCs, and liver DRM TAMRA-A $\beta_{1-42}$ levels after TAMRA-A $\beta_{1-42}$ infusion in vivo*

TAMRA-A $\beta_{1-42}$  was found in DRMs isolated from RBCs of TAMRA-A $\beta_{1-42}$  infused rats. The TAMRA-A $\beta_{1-42}$  level in the DRMs of RBCs was again higher in DHA-pretreated rats (Figure 4C). More interestingly, the levels of plasma TAMRA-A $\beta_{1-42}$  were significantly decreased in DHA-pretreated rats (Figure 4A), as compared with those of control rats, with a corresponding increase in the levels of TAMRA-A $\beta_{1-42}$  in DRMs isolated from the livers of DHA-pretreated rats (Figure 4B). The decreases in the plasma levels of TAMRA-A $\beta_{1-42}$  were accompanied by rises in the protein levels of cathepsin D (protease activities) of both RBC ghosts (see Supplementary file 6) and liver (Figure 4D).

## **4. Discussion**

The objective of this study was to investigate: i) whether dietary DHA affects the interactions between A $\beta_{1-42}$  and RBCs and hemolysis, and then ii) the molecular mechanism involved in this effect. This study showed that the RBC undergoes a morphological alteration caused by interactions with A $\beta$ , in agreement with previous studies [1,28]. Dietary pre-administration of DHA reduced the hemolysis and increased the accumulation of A $\beta$ s in RBC and liver lipid rafts, and RBC and hepatic cathepsin D levels. These changes may contribute to the clearance of circulatory A $\beta_{1-42}$ .

The hemolysis conferred by TAMRA-A $\beta_{1-42}$  and/or unlabeled A $\beta_{1-42}$  was significantly lower in the RBCs of DHA-pretreated rats. Oxidative and structure-disrupting events induced

by A $\beta$  at the level of the plasma membrane, therefore, appear to represent initiating events in hemolytic cascades induced by A $\beta$ . The reduction of hemolysis in the RBCs of DHA-pretreated rats may be due to increased levels of antioxidants, including GSH, decreased LPO, and ROS in the RBCs (see additional file 6). Consistently with other reports [1,3], hemolysis was inhibited in the presence of the antioxidant  $\alpha$ -tocopherol.

The RBC concentration of A $\beta_{1-42}$  increases in elderly people [1]. In addition, it has been reported that A $\beta_{1-40}$  and A $\beta_{1-42}$  binds with, and/or is taken up, by RBCs after *in vitro* incubation [6,29]. Moreover, A $\beta_{1-42}$  interacts with RBC more avidly than A $\beta_{1-40}$  [1,6,30], because of its increased propensity for aggregation [20] and two additional hydrophobic amino acids at the C-terminus of A $\beta_{1-42}$  that facilitates penetration into the RBC bilayer [31]. In this study, microscopy revealed a drastic change in RBC morphology by A $\beta_{1-42}$ , which was associated with numerous blobs and diffused membranes with multiple leaks, confirming interaction between RBC and A $\beta$ s. These results were consistent with increased hemolysis by A $\beta_{1-42}$  treatment. Moreover, during hemolysis, the interactions between RBC membranes and A $\beta_{1-42}$  were evident from the presence of TAMRA-A $\beta_{1-42}$  at the vicinity of the RBCs.

We hypothesized that A $\beta$  bind with the DRMs in RBCs; however, the identity of the structural domains of the DRMs that bind to A $\beta_{1-42}$  has remained obscure. The presence of DRMs in RBCs even *in vivo* is well documented [32]. Recent evidence suggests that A $\beta$  oligomers confer neurotoxicity by causing aberrant clustering of lipid raft proteins [33]. In our study, TAMRA-A $\beta_{1-42}$  consistently bound to DRMs *in vitro* and *in vivo*. Considering that the binding of TAMRA-A $\beta$  vs. unlabeled A $\beta$ s was competitive, we showed that binding of A $\beta$ s to DRMs is to some extent specific. The results were qualitatively consistent with available published findings that A $\beta$ s accumulate appreciably in the DRMs of RBCs. We considered the following points to assess the mechanisms of the interaction between A $\beta$  and RBCs; (i) the RBCs have the only plasma membrane; hence, there is no turnover of plasma

membrane proteins from intracellular sources, (ii) mature RBCs are unable to synthesize new proteins, and (iii) RBC is a terminally differentiated cell that completely lacks endocytic capability. Thus, the events triggering binding of  $A\beta_{1-42}$  to RBCs must derive from pre-existing proteins. In other words, the endocytosis-independent mechanism must exist for the interaction with the extracellular  $A\beta$ s that are to be taken up and/or bound on the surface of RBCs, as reported earlier [1,29].

DRM vesicles displayed  $A\beta$ s putatively bound on their surface and/or accumulated inside them (Figure 2). The above findings suggest that DRMs proteins are engaged in interaction with the  $A\beta$ s. We accordingly speculate that one of the candidates that affect the interactions between  $A\beta$ s and DRMs is caveolin-1. Consistently with this notion, the presence of caveolin-1 has been reported in RBC [34]. Irrespective of the mechanism(s), i)  $A\beta$  binds with caveolin-1-containing lipid rafts of RBCs and is subjected to protease degradative enzymes present on or bound to their own surfaces, and/or ii) RBCs, via their lipid raft pockets, transport and deliver the  $A\beta$ s to the liver for detoxification by hepatic proteolytic enzymes such as cathepsin D. However, TAMRA- $A\beta$  was not enriched/associated with DRMs uniformly. Although the exact reason for this is unclear, we hypothesize that  $A\beta_{1-42}$  accumulates in caveolin 1-containing DRMs. The highest caveolin1 levels were present in DRMS in fraction 3 of the sucrose gradient. Therefore, it is possible that there are subsets of DRMs that harbor varying amounts of caveolin 1, and hence TAMRA- $A\beta_{1-42}$ . We speculate that this might explain why TAMRA was not enriched in the DRMs uniformly. DHA increased DRM fluidity (see Supplementary file 8) with concomitant decreases of cholesterol and increases of DHA levels in DRM domains (Table 1). Increased membrane fluidity facilitates endocytosis-like events. DHA increases both lateral and translational membrane fluidity of the lipid bilayer [18,25]. Therefore, it is very likely that a DHA-induced increase in fluidity accelerates the lateral movement of individual rafts within DRMs. Thus, it can be

speculated that DHA might have facilitated the accommodation of caveolin-1 in the lipid raft platforms and/or stabilized the association between caveolin-1 and A $\beta$ , thereby concentrating them for degradation. This speculation is consistent with the results of real-time monitoring by FCS of the interactions and dynamic behaviors of TAMRA-A $\beta$ <sub>1-42</sub> with the DRMs of RBCs of DHA-pretreated rats. In the present study, we also demonstrated that levels of caveolin-1 increased, accompanied with increased TAMRA-A $\beta$ <sub>1-42</sub> levels in the DRMs of RBCs and liver of the DHA-pretreated rats. The levels of A $\beta$ s in the plasma were decreased. These results indicate that DHA increased the binding of A $\beta$ <sub>1-42</sub> to DRMs in RBCs via caveolin-1-rich lipid rafts or caveolae of the DRMs and were transported to the liver, which decreased the plasma level of TAMRA-A $\beta$ <sub>1-42</sub> after infusion.

## 5. Conclusions

The results of the present study are consistent with the hypothesis that the enrichment of DHA in RBCs might ameliorate the plasma burden of amyloids. In conclusion, alterations in morphology originated from modifications caused by toxic oligomeric A $\beta$  interactions with RBCs, and these interactions involved caveolin-1-rich lipid rafts. However, these RBC-disrupting interactions were ameliorated by the pre-administration of DHA by antioxidation and change in the membrane properties of RBC. This is the first report that DHA enhances the clearance of A $\beta$ <sub>1-42</sub> in the plasma and suggests that DHA supplementation can help to prevent the risk of AD.

## Acknowledgement

It is a pleasure to acknowledge Harima Foods, Inc. (Osaka, Japan) for its generous gift of DHA-95E as an ethyl ester derivative of all cis-4,7,10,13,16,19-docosahexaenoic acid. This study was supported, in part, by a Grant-in-Aid for Scientific Research (C) (#23500955 to

MH) and by a Grant-in-Aid for Young Scientists (B) (#24790234 to MK) from the Ministry of Education, Science and culture of Japan.

ACCEPTED MANUSCRIPT

**References**

- [1] T. Kiko, K. Nakagawa, A. Satoh, T. Tsuduki, K. Furukawa, H. Arai, T. Miyazawa, Amyloid beta levels in human red blood cells. *PLoS One* **7** (2012) :e49620.
- [2] G.J. Bosman, I.G. Bartholomeus, A.J. de Man, van P.J. Kalmthout, W.J. de Grip, Erythrocyte membrane characteristics indicate abnormal cellular aging in patients with Alzheimer's disease, *Neurobiol Aging* **12** (1991)13-18.
- [3] M. P. Mattson, J.G. Begley, R.J. Mark, K. Furukawa,  $A\beta_{25-35}$  induces rapid lysis of red blood cells: contrast with  $A\beta_{1-42}$  and examination of underlying mechanisms, *Brain Res.* **771** (1997)147-153.
- [4] N. Mohandas, J.A. Chasis, Red blood cell deformability, membrane material properties and shape: regulation by transmembrane, skeletal and cytosolic proteins and lipids, *Semin. Hematol* **30** (1993)171-92.
- [5] C.W. Wu, P.C. Liao, L. Yu, S.T. Wang, S.T. Chen, C.M. Wu, Y.M. Kuo, Hemoglobin promotes  $A\beta$  oligomer formation and localizes in neurons and amyloid deposits. *Neurobiol. Dis.* **17** (2004)367-377.
- [6] Y.M. Kuo, T.A. Kokjohn, W. Kalback, D. Luehrs, D.R. Galasko, N. Chevallier, E.H. Koo, M.R. Emmerling, A.E. Roher, Amyloid-beta peptides interact with plasma proteins and erythrocytes: implications for their quantitation in plasma, *Biochem. Biophys. Res. Commun.* **268** (2000)750-756.
- [7] K. Nakagawa, T. Kiko, S. Kuriwada, T. Miyazawa, F. Kimura, T. Miyazawa, Amyloid beta induces adhesion of erythrocytes to endothelial cells and affects endothelial viability and functionality, *Biosci. Biotechnol. Biochem.* **75** (2011)2030-2033.
- [8] F. Galbiati, B. Razani, M.P. Lisanti, Emerging themes in lipid rafts and caveolae, *Cell* **106** (2001) 403-411.

- [9] K.G. Rothberg, J.E. Heuser, W.C. Donzell, Y.S. Ying, J.R. Glenney, R.G. Anderson, Caveolin, a protein component of caveolae membrane coats, *Cell* 68 (1992) 673-682.
- [10] D.A. Brown, E. London, Structure and function of sphingolipid- and cholesterol-rich membrane rafts, *J. Biol. Chem.* 275 (2000)17221-17224.
- [11] L. J. Pike, Lipid rafts: bringing order to chaos. *J. Lipid Res.* 44 (2003) 655–667.
- [12] A. Pralle, P. Keller, E.L. Florin, K. Simons, J.K. Horber, Sphingolipid-cholesterol rafts diffuse as small entities in the plasma membrane of mammalian cells, *J. Cell. Biol.* 148 (2000) 997-1008.
- [13] N. Kahya, D. Scherfeld, K. Bacia, B. Poolman, P. Schwille, Probing lipid mobility of raft-exhibiting model membranes by fluorescence correlation spectroscopy. *J. Biol. Chem.* 278 (2003) 28109-28115.
- [14] K. Bacia, D. Scherfeld, N. Kahya, P. Schwille, Fluorescence correlation spectroscopy relates rafts in model and native membranes. *Biophys. J.* 87 (2004) 1034-1043.
- [15] S.A. Kim, K.G. Heinze, P. Schwille, Fluorescence correlation spectroscopy in living cells. *Nat. Methods* 4 (2007) 963-973.
- [16] W. Wang, L. Shinto, W.E. Connor, J.F.Quinn: Nutritional biomarkers in Alzheimer's disease: the association between carotenoids, n-3 fatty acids, and dementia severity, *J. Alzheimers Dis.* 13 (2008) 31-38.
- [17] M. Hashimoto, S. Hossain, T. Shimada, K. Sugioka, H. Yamasaki, Y. Fujii, Y. Ishibashi, J. Oka, O Shido, Docosahexaenoic acid provides protection from impairment of learning ability in Alzheimer's disease model rats, *J. Neurochem.* 81 (2002)1084-1091.
- [18] M. Hashimoto, S Hossain, T Shimada, O Shido, Docosahexaenoic acid-induced protective effect against impaired learning in amyloid beta-infused rats is associated

- with increased synaptosomal membrane fluidity, *Clin. Exp. Pharmacol. Physiol.* 33 (2006) 934-939.
- [19] M. Hashimoto, H. Shahdat, S. Yamashita, M. Katakura, Y. Tanabe, H. Fujiwara, S. Gamoh, T. Miyazawa, N. Arai, T. Shimada, Docosahexaenoic acid disrupts in vitro amyloid beta(1-40) fibrillation and concomitantly inhibits amyloid levels in cerebral cortex of Alzheimer's disease model rats, *J. Neurochem.* 107 (2008)1634-1646.
- [20] S. Hossain, M. Hashimoto, M. Katakura, K. Miwa, T. Shimada, O. Shido, Mechanism of docosahexaenoic acid-induced inhibition of in vitro A $\beta$ <sub>1-42</sub> fibrillation and A $\beta$ <sub>1-42</sub>-induced toxicity in SH-SY5Y cells, *J. Neurochem.* 111 (2009)568-579.
- [21] D.A. Brown, J.K. Rose, Sorting of GPI-anchored proteins to glycolipid-enriched membrane subdomains during transport to the apical cell surface, *Cell* 68 (1992) 533-544.
- [22] A.M. Fra, E. Williamson, K. Simons, R.G. Parton, Detergent-insoluble glycolipid microdomains in lymphocytes in the absence of caveolae, *J. Biol. Chem.* 269 (1994) 30745-30748.
- [23] L. Abrami, M. Fivaz, P.E. Glauser, R.G. Parton, F.G. van der Goot, A pore-forming toxin interacts with a GPI-anchored protein and causes vacuolation of the endoplasmic reticulum, *J. Cell Biol.* 140 (1998)525-540.
- [24] G. P. Lim, F. Calon, T. Morihara, F. Yang, B. Teter, O. Ubeda, Jr. N. Salem, S.A. Frautschy, G.M. Cole, A diet enriched with the omega-3 fatty acid docosahexaenoic acid reduces amyloid burden in an aged Alzheimer mouse model. *J. Neurosci.* 25 (2005) 3032-3040.
- [25] M. Hashimoto, M. S. Hossain, T. Shimada, H. Yamasaki, Y. Fujii, O. Shido, Effects of docosahexaenoic acid on annular lipid fluidity of the rat bile canalicular plasma membrane, *J. Lipid Res.* 42 (2001),1160-1168.

- [26] M.S. Hossain, M. Hashimoto, S. Gamoh, S Masumura, Antioxidative effects of docosahexaenoic acid in the cerebrum versus cerebellum and brainstem of aged hypercholesterolemic rats, *J. Neurochem.* 72 (1999)1133-1138.
- [27] P.J. Hissin, R. Hilf, A fluorometric method for determination of oxidized and reduced glutathione in tissues, *Anal. Biochem.* 74 (1976) 214-226.
- [28] J.G. Mohanty, H.D. Shukla, J.D. Williamson, L.J. Launer, S. Saxena, J.M. Rifkind, Alterations in the red blood cell membrane proteome in alzheimer's subjects reflect disease-related changes and provide insight into altered cell morphology. *Proteome Sci.* 8 (2010)11.
- [29] R. Jayakumar, J.W. Kusiak, F.J. Chrest, A.A. Demehin, J. Murali, R.P. Wersto, E. Nagababu, L. Ravi, J.M. Rifkind, Red cell perturbations by amyloid beta-protein. *Biochim. Biophys. Acta* 1622 (2003) 20-28.
- [30] K. Nakagawa, T. Kiko, T. Miyazawa, P. Sookwong, T. Tsuduki, A. Satoh, T. Miyazawa, Amyloid  $\beta$ -induced erythrocytic damage and its attenuation by carotenoids. *FEBS Lett* 585 (2011)1249-1254.
- [31] T. Pillot, M. Goethals, B. Vanloo, C. Talussot, R. Brasseur, J. Vandekerckhove, M. Rosseneu, L. Lins, Fusogenic properties of the C-terminal domain of the Alzheimer beta-amyloid peptide. *J. Biol. Chem.* 271(1996) 28757-28765.
- [32] I. Mikhalyov, A. Samsonov, Lipid raft detecting in membranes of live erythrocytes. *Biochim. Biophys. Acta* 1808 (2011) 1930-1939.
- [33] J.V. Rushworth, N.M. Hooper, Lipid Rafts: Linking Alzheimer's Amyloid-beta Production, Aggregation, and Toxicity at Neuronal Membranes. *Int. J. Alzheimers Dis.* 2011 (2010) 603052.
- [34] B. Ozuyaman, M. Grau, M. Kelm, M.W. Merx, P. Kleinbongard, RBC NOS: regulatory mechanisms and therapeutic aspects. *Trends Mol. Med.* 14(2008) 314-322.

**Table legend**

**Table1.** Cholesterol ( $\mu\text{g}/\text{mg}$  protein) and fatty acid compositions (mol%) of plasma, RBC ghost and DRMs.

Results are mean  $\pm$  SE (standard error of mean,  $n = 8-10$ ). \*  $P < 0.05$ . F1 vs DHA (Student's t-test). RBC, red blood cell; DRMs, detergent-resistant membranes; PLA, Palmitic acid, C16:0; STA, Stearic acid, C18:0; OLA, Oleic acid, C18:1 (n-9); LLA, Linoleic acid, C18:2 (n-6); LNA, Linoleinic acid, C18:3 (n-3); AA, Arachidonic acid, C20:4 (n-6); EPA, Eicosapentaenoic acid C20:5 (n-3); DPA, Docosapentaenoic acid, C22:5 (n-3); DHA, Docosahexaenoic acid, C22:6 (n-3); LGA, Lignoceric acid, C24:0; NVA, Nervonic acid, C24:1; CHOL, Total cholesterol. ND, Not determined.

**Figure legends****Figure 1.**

**Panel 1:** Effect of  $A\beta_{1-42}$  on RBC morphology and hemolysis. A, B: Represents effects of unlabeled  $A\beta_{1-42}$ , while C,D,E represent that of the labelled Abeta (TAMRA- $A\beta_{1-42}$ ), as viewed in the confocal laser microscopic field. Thus numerous blobs, bulges, and diffuse membranes with multiple leakages were seen in  $A\beta_{1-42}$ -treated RBCs (B, inset B1, C, D, E). In contrast, control RBCs ( $A\beta_{1-42}$ -untreated RBCs) did not become permeated and did not reveal membrane discontinuities, but it exhibited clear demarcations of their membranes (A, inset A1). The results were consistent with increased leakage of hemoglobin from  $A\beta_{1-42}$ -treated control RBCs (F).

**Panel 2:** Confocal laser microscopic views of detergent-resistant membranes (DRMs) incubated without (A, control) or with TAMRA- $A\beta_{1-42}$  (B). The DRMs, which spontaneously

formed membranous vesicles, also appeared as swollen red cells in the confocal field. Immunofluorescence of TAMRA-A $\beta_{1-42}$  was clearly discernible at the surface and/or inside the DRMs structures (B, C), as compared with the untreated (A) DRMS vesicles. (C): immunofluorescence in the z-direction of the vesicles.

**Panel 3:** Transmission electron microscopic (TEM) views of A $\beta_{1-42}$ -incubated DRMs samples. Some A $\beta_{1-42}$ -fibers were visible in, though not exclusively, the sacs of the DRMs (A, B, C, D, E; black arrows indicate the presence of amyloid fibers). Some DRMs were found as grape-like clusters at or around (the branches of) fibers (F, G). H: Perseverance of DRMs-like vesicles in RBC ghost preparations stored at 4°C for 2 days.

## Figure 2.

**Panel 1:** Effects of dietary preadministration of DHA on the binding of A $\beta_{1-42}$  on the DRMs of RBCs. **A:** Saturation of DRM-bound TAMRA-A $\beta_{1-42}$  was obtained as a function of TAMRA-A $\beta_{1-42}$  concentration. Control DRMs were incubated overnight with different concentrations of TAMRA-A $\beta_{1-42}$  (0–10 nM). Each data point represents the mean of triplicate determinations of at least three separate measurements. **B:** The effects of DHA on the relative TAMRA-A $\beta_{1-42}$  occupancy of DRMs after overnight incubation were evaluated at a fixed (5 nM). The DRMs of RBCs of DHA rats had significantly increased (occupancy) levels of TAMRA-A $\beta_{1-42}$  than those of control rats. **C:** Competitive binding/occupancy of TAMRA-A $\beta_{1-42}$  (5 nM) to DRMs vesicles with access of unlabeled A $\beta_{1-42}$  (0–10  $\mu$ M). Bound TAMRA-A $\beta_{1-42}$  was displaced by unlabeled TAMRA-A $\beta_{1-42}$ . The DHA-enriched DRMs had more (displaced) unlabeled A $\beta_{1-42}$ , as measured by ELISA. **D:** The affinity of the Abetas for DRMs was also calculated by fitting the data to a one-site-competition equation [ $Y = \text{Bottom} + (\text{Top} - \text{Bottom}) / (1 + 10^{(X - \text{LogEC}_{50})})$ ], where  $X = \log(\text{concentration})$  and  $Y = \text{bound/unbound}$ . EC<sub>50</sub> values in the DRMs of F1 control and DHA rats were, respectively,

9.55 and 6.78 nM. \*  $P < 0.05$ . F1 vs. DHA (Student's  $t$ -test).

**Panel 2:** Autocorrelation ( $G(t)$ ) curves of fluorescence fluctuations of free 5-6-carboxytetramethylrhodamine (TAMRA) dye (**A**); TAMRA- $A\beta_{1-42}$  free in solution, TAMRA- $A\beta_{1-42}$  + DRMs of RBCs of F1 control and DHA-preadministered rats (**B**) after overnight incubation. The autocorrelation functions of free TAMRA and TAMRA- $A\beta_{1-42}$  alone in buffer solution only were best fitted with a one-component analysis model, and the respective diffusion times were estimated at approximately 100 and 260  $\mu$ s (red fitting curve). The autocorrelation function of TAMRA- $A\beta_{1-42}$  mixed with DRMs (TAMRA- $A\beta_{1-42}$  + DRMS) samples was best fitted with a two-component analysis model by fixing the diffusion time ( $\tau_1$ ) of the free fraction TAMRA- $A\beta_{1-42}$  at approximately 260  $\mu$ s (red fitting curve) and gave rise to the second component ( $\tau_2$ ) of diffusion time, with respective values of  $3228 \pm 300$  and  $3485 \pm 285$   $\mu$ s in the DRMs of F1 control and DHA rats.

**Figure 3.** Effect of dietary pre-administration of docosahexaenoic acid on caveolin-1 levels in lipid rafts containing DRMs of F1 control and DHA RBCs. **A:** Levels of caveolin-1 in DRM fractions obtained by high-speed centrifugation (30 min, 4°C, at 55,000 rpm in a TLA55 Beckman rotor). **B:** Levels of caveolin-1 in purified DRM fractions obtained from 5%, 35%, and 40% sucrose gradient centrifugations. Fraction 1 represents fraction 1, above the 5% sucrose; Fraction 2 represents fraction 2 from the interface between 5% and 30%; Fraction 3 represents the fraction from the interface between 35% and 40%; and Fraction 4 represents fraction 4, the sediment below the 40% sucrose layer. \*  $P < 0.05$ . F1 vs DHA (Student's  $t$ -test).

**Figure 4.** Effects of oral pre-administration of DHA on the levels of infused TAMRA- $A\beta_{1-42}$  into blood plasma (A), DRMs of liver (B) and RBC (C), and hepatic cathepsin D protease

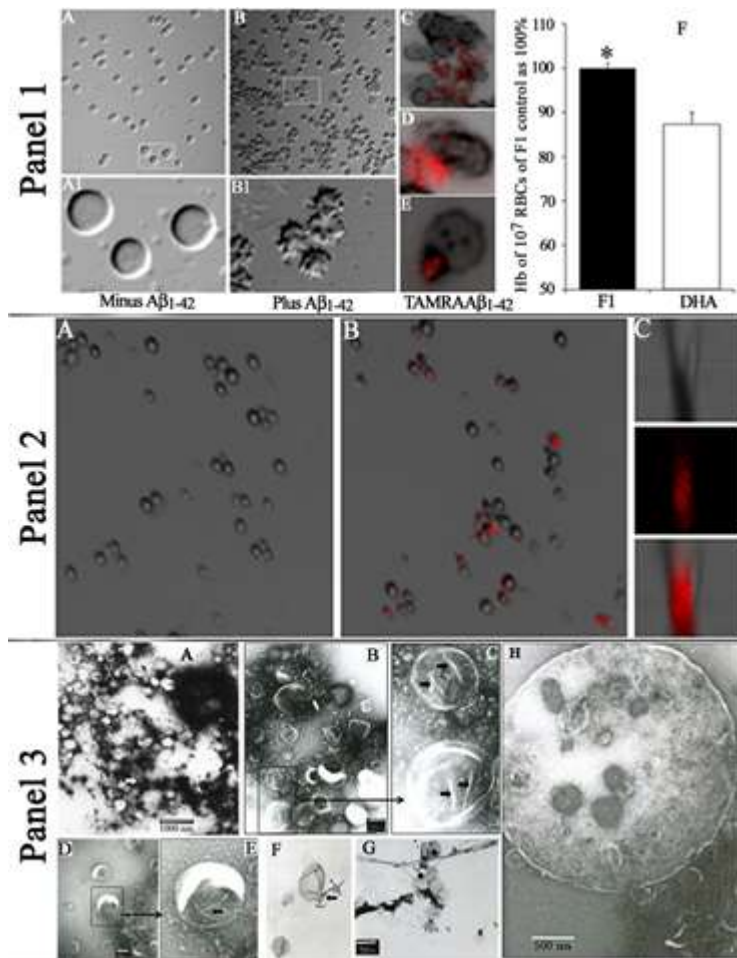
enzyme (D); cathepsin proteins were measured in the post-nuclear fraction of liver homogenates. \*  $P < 0.05$ . F1 vs. DHA (Student's t-test).

ACCEPTED MANUSCRIPT

**Table1.** Cholesterol ( $\mu\text{g}/\text{mg}$  protein) and fatty acid compositions (mol%) of plasma, RBC ghost and DRMs

	Plasma		RBC ghost		DRMs	
	F1	DHA	F1	DHA	F1	DHA
PLA	25.0 $\pm$ 0.5	26.0 $\pm$ 0.6	36.0 $\pm$ 1.1	36.5 $\pm$ 0.7	48.6 $\pm$ 0.8	48.0 $\pm$ 1.2
STA	12.0 $\pm$ 0.3	11.1 $\pm$ 0.4	21.3 $\pm$ 0.9	21.2 $\pm$ 1.0	19.0 $\pm$ 0.2	18.0 $\pm$ 1.0
OLA	16.5 $\pm$ 0.5	15.2 $\pm$ 0.7	8.8 $\pm$ 0.1	8.6 $\pm$ 0.3	7.0 $\pm$ 1.1	5.2 $\pm$ 0.3*
LLA	12.6 $\pm$ 0.3	19.3 $\pm$ 0.5*	5.2 $\pm$ 0.2	8.0 $\pm$ 0.3*	3.7 $\pm$ 0.1	4.5 $\pm$ 0.8
LNA	0.13 $\pm$ 0.01	0.20 $\pm$ 0.01*	0.05 $\pm$ 0.01	0.05 $\pm$ 0.01	0.03 $\pm$ 0.01	0.02 $\pm$ 0.01
AA	30.4 $\pm$ 1.0	12.0 $\pm$ 0.5*	22.4 $\pm$ 1.7	15.0 $\pm$ 0.8*	14.0 $\pm$ 0.4	7.5 $\pm$ 1.8*
EPA	0.14 $\pm$ 0.01	2.70 $\pm$ 0.16*	0.11 $\pm$ 0.04	0.80 $\pm$ 0.10*	0.05 $\pm$ 0.01	0.40 $\pm$ 0.08
DPA	0.20 $\pm$ 0.02	0.60 $\pm$ 0.10*	0.40 $\pm$ 0.05	0.70 $\pm$ 0.05*	0.30 $\pm$ 0.02	0.40 $\pm$ 0.10
LGA	0.50 $\pm$ 0.01	0.40 $\pm$ 0.01	2.5 $\pm$ 0.1	2.9 $\pm$ 0.2	3.1 $\pm$ 0.3	3.4 $\pm$ 0.7
DHA	1.7 $\pm$ 0.1	12.1 $\pm$ 0.8*	1.3 $\pm$ 0.2	4.6 $\pm$ 0.4*	1.2 $\pm$ 0.1	2.5 $\pm$ 0.6*
NVA	0.40 $\pm$ 0.01	0.20 $\pm$ 0.01*	2.0 $\pm$ 0.1	1.8 $\pm$ 0.1	2.8 $\pm$ 0.3	2.0 $\pm$ 0.5
CHOL	ND	ND	522 $\pm$ 45	416 $\pm$ 26*	268 $\pm$ 15	221 $\pm$ 4*

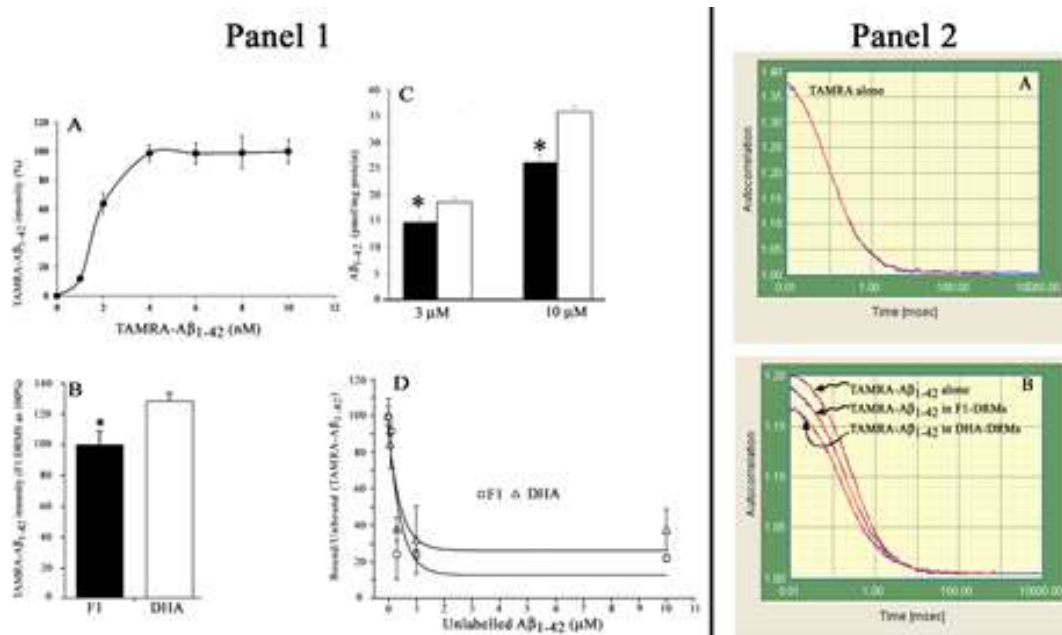
Results are mean  $\pm$  SE (standard error of mean, n = 8-10). \*  $P < 0.05$ . F1 vs DHA (Student's t-test). RBC, red blood cell; DRMs, detergent-resistant membranes; PLA, Palmitic acid, C16:0; STA, Stearic acid, C18:0; OLA, Oleic acid, C18:1 (n-9); LLA, Linoleic acid, C18:2 (n-6); LNA, Linoleic acid, C18:3 (n-3); AA, Arachidonic acid, C20:4 (n-6); EPA, Eicosapentaenoic acid C20:5 (n-3); DPA, Docosapentaenoic acid, C22:5 (n-3); DHA, Docosahexaenoic acid, C22:6 (n-3); LGA, Lignoceric acid, C24:0; NVA, Nervonic acid, C24:1; CHOL, Total cholesterol. ND, Not determined.



**Figure 1. Panel 1:** Effect of Aβ<sub>1-42</sub> on RBC morphology and hemolysis. A, B: Represents effects of unlabeled Aβ<sub>1-42</sub>, while C, D, E represent that of the labelled Abeta (TAMRA-Aβ<sub>1-42</sub>), as viewed in the confocal laser microscopic field. Thus numerous blobs, bulges, and diffuse membranes with multiple leakages were seen in Aβ<sub>1-42</sub>-treated RBCs (B, inset B1, C, D, E). In contrast, control RBCs (Aβ<sub>1-42</sub>-untreated RBCs) did not become permeated and did not reveal membrane discontinuities, but it exhibited clear demarcations of their membranes (A, inset A1). The results were consistent with increased leakage of hemoglobin from Aβ<sub>1-42</sub>-treated control RBCs (F).

**Panel 2:** Confocal laser microscopic views of detergent-resistant membranes (DRMs) incubated without (A, control) or with TAMRA-Aβ<sub>1-42</sub> (B). The DRMs, which spontaneously formed membranous vesicles, also appeared as swollen red cells in the confocal field. Immunofluorescence of TAMRA-Aβ<sub>1-42</sub> was clearly discernible at the surface and/or inside the DRMs structures (B, C), as compared with the untreated (A) DRMS vesicles. (C): immunofluorescence in the z-direction of the vesicles.

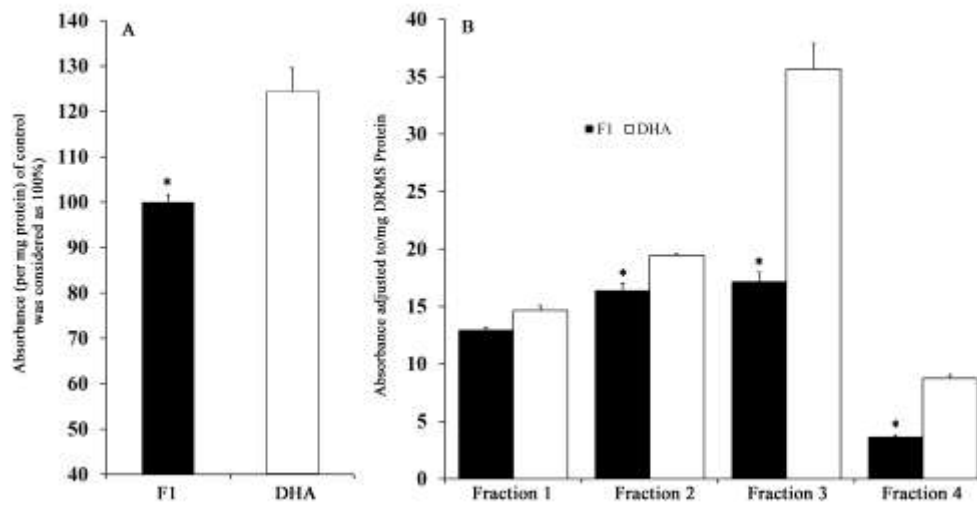
**Panel 3:** Transmission electron microscopic (TEM) views of Aβ<sub>1-42</sub>-incubated DRMs samples. Some Aβ<sub>1-42</sub>-fibers were visible in, though not exclusively, the sacs of the DRMs (A, B, C, D, E; black arrows indicate the presence of amyloid fibers). Some DRMs were found as grape-like clusters at or around (the branches of) fibers (F, G). H: Perseverance of DRMs-like vesicles in RBC ghost preparations stored at 4°C for 2 days.



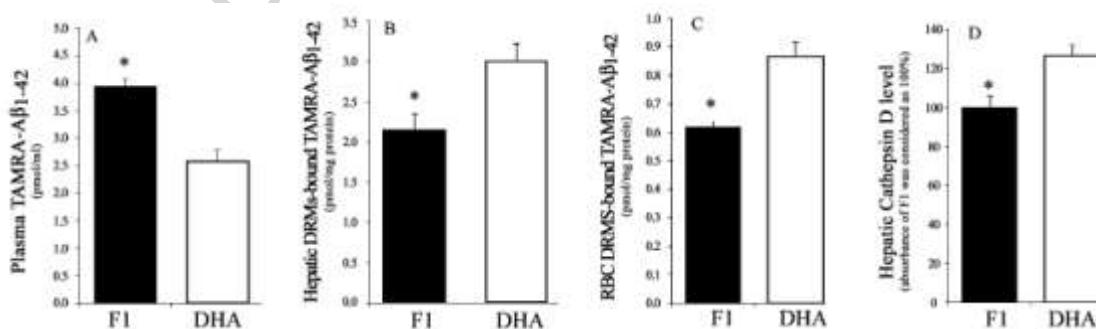
**Figure 2.**

**Panel 1:** Effects of dietary preadministration of DHA on the binding of A $\beta_{1-42}$  on the DRMs of RBCs. **A:** Saturation of DRM-bound TAMRA-A $\beta_{1-42}$  was obtained as a function of TAMRA-A $\beta_{1-42}$  concentration. Control DRMs were incubated overnight with different concentrations of TAMRA-A $\beta_{1-42}$  (0–10 nM). Each data point represents the mean of triplicate determinations of at least three separate measurements. **B:** The effects of DHA on the relative TAMRA-A $\beta_{1-42}$  occupancy of DRMs after overnight incubation were evaluated at a fixed (5 nM). The DRMs of RBCs of DHA rats had significantly increased (occupancy) levels of TAMRA-A $\beta_{1-42}$  than those of control rats. **C:** Competitive binding/occupancy of TAMRA-A $\beta_{1-42}$  (5 nM) to DRMs vesicles with access of unlabeled A $\beta_{1-42}$  (0–10  $\mu$ M). Bound TAMRA-A $\beta_{1-42}$  was displaced by unlabeled TAMRA-A $\beta_{1-42}$ . The DHA-enriched DRMs had more (displaced) unlabeled A $\beta_{1-42}$ , as measured by ELISA. **D:** The affinity of the Abetas for DRMs was also calculated by fitting the data to a one-site-competition equation [ $Y = \text{Bottom} + (\text{Top} - \text{Bottom}) / (1 + 10^{(X - \text{LogEC}_{50})})$ ], where  $X = \log(\text{concentration})$  and  $Y = \text{bound/unbound}$ . EC<sub>50</sub> values in the DRMs of F1 control and DHA rats were, respectively, 9.55 and 6.78 nM. \*  $P < 0.05$ . F1 vs. DHA (Student's t-test).

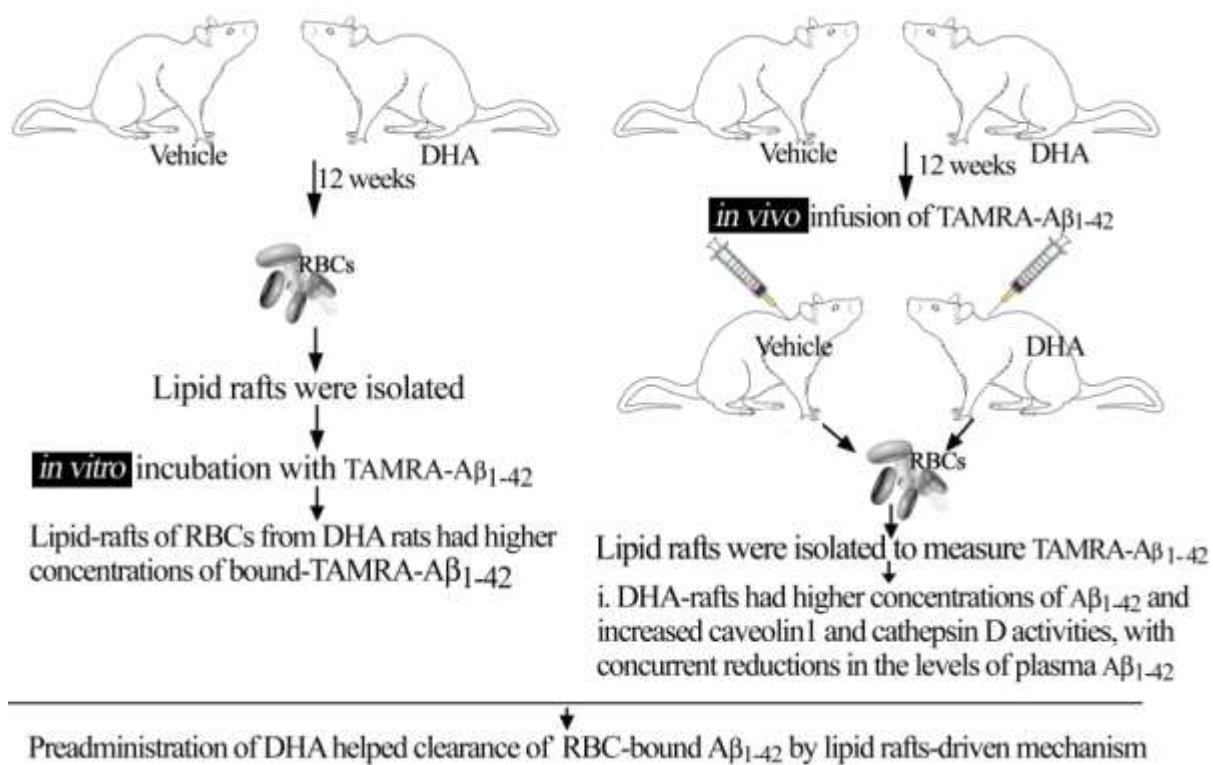
**Panel 2:** Autocorrelation (Gt) curves of fluorescence fluctuations of free 5-6-carboxytetramethylrhodamine (TAMRA) dye (A); TAMRA-A $\beta_{1-42}$  free in solution, TAMRA-A $\beta_{1-42}$  + DRMs of RBCs of F1 control and DHA-preadministered rats (B) after overnight incubation. The autocorrelation functions of free TAMRA and TAMRA-A $\beta_{1-42}$  alone in buffer solution only were best fitted with a one-component analysis model, and the respective diffusion times were estimated at approximately 100 and 260  $\mu$ s (red fitting curve). The autocorrelation function of TAMRA-A $\beta_{1-42}$  mixed with DRMs (TAMRA-A $\beta_{1-4}$  + DRMS) samples was best fitted with a two-component analysis model by fixing the diffusion time ( $\tau_1$ ) of the free fraction TAMRA-A $\beta_{1-42}$  at approximately 260  $\mu$ s (red fitting curve) and gave rise to the second component ( $\tau_2$ ) of diffusion time, with respective values of  $3228 \pm 300$  and  $3485 \pm 285$   $\mu$ s in the DRMs of F1 control and DHA rats.



**Figure 3.** Effect of dietary pre-administration of docosahexaenoic acid on caveolin-1 levels in lipid rafts containing DRMs of F1 control and DHA RBCs. **A:** Levels of caveolin-1 in DRM fractions obtained by high-speed centrifugation (30 min, 4°C, at 55,000 rpm in a TLA55 Beckman rotor). **B:** Levels of caveolin-1 in purified DRM fractions obtained from 5%, 35%, and 40% sucrose gradient centrifugations. Fraction 1 represents fraction 1, above the 5% sucrose; Fraction 2 represents fraction 2 from the interface between 5% and 30%; Fraction 3 represents the fraction from the interface between 35% and 40%; and Fraction 4 represents fraction 4, the sediment below the 40% sucrose layer. \*  $P < 0.05$ . F1 vs DHA (Student's  $t$ -test).



**Figure 4.** Effects of oral pre-administration of DHA on the levels of infused TAMRA-A $\beta_{1-42}$  into blood plasma (A), DRMs of liver (B) and RBC (C), and hepatic cathepsin D protease enzyme (D); cathepsin proteins were measured in the post-nuclear fraction of liver homogenates. \*  $P < 0.05$ . F1 vs. DHA (Student's  $t$ -test).



Graphical abstract